0026-895X/08/7303-758–768$20.00
MOLECULAR PHARMACOLOGY
Copyright © 2008 The American Society for Pharmacology and Experimental Therapeutics
Mol Pharmacol 73:758–768, 2008

Vol. 73, No. 3
43208/3310644
Printed in U.S.A.

Small-Molecule Screen Identifies Inhibitors of a Human Intestinal Calcium-Activated Chloride Channel

Ricardo De La Fuente, Wan Namkung, Aaron Mills, and A. S. Verkman

Departments of Medicine and Physiology, Cardiovascular Research Institute, University of California, San Francisco, California

ABSTRACT

Calcium-activated chloride channels (CaCCs) are widely expressed in mammalian tissues, including intestinal epithelia, where they facilitate fluid secretion. Potent, selective CaCC inhibitors have not been available. We established a high-throughput screen for identification of inhibitors of a human intestinal CaCC based on inhibition of ATP/carbachol-stimulated iodide influx in HT-29 cells after lentiviral infection with the yellow fluorescent halide-sensing protein YFP-H148Q/I152L. Screening of 50,000 diverse, drug-like compounds yielded six classes of putative CaCC inhibitors, two of which, 3-acyl-2-aminothiophenes and 5-aryl-2-aminothiazoles, inhibited by >95% iodide influx in HT-29 cells in response to multiple calcium-elevating agonists, including thapsigargin, without inhibition of calcium elevation, calcium-calmodulin kinase II activation, or cystic fibrosis transmembrane conductance regulator chloride channels. These compounds also inhibited calcium-dependent chloride secretion in T84 human intestinal epithelial cells. Patch-clamp analysis indicated inhibition of CaCC gating, which, together with the calcium-calmodulin data, suggests that the inhibitors target the CaCC directly. Structure-activity relationships were established from analysis of more than 1800 analogs, with IC_{50} values of the best analogs down to ~1 μM. Small-molecule CaCC inhibitors may be useful in pharmacological dissection of CaCC functions and in reducing intestinal fluid losses in CaCC-mediated secretory diarrheas.

There are at least five distinct classes of mammalian Cl^- channels, including the cystic fibrosis transmembrane conductance regulator (CFTR), CLC-type voltage-sensitive Cl^- channels, ligand-gated (GABA and glycine) Cl^- channels, volume-sensitive Cl^- channels, and calcium-activated Cl^- channels (CaCCs) (reviewed in Eggermont, 2004; Hartzell et al., 2005a). The molecular identities of epithelial cell CaCCs remain unclear, with potential candidates including *bestrophins* (Best1-Best4), CLCs of the *CKCA* family, and products of the recently described *tweety* gene (Hartzell et al., 2005b; Loewen and Forsyth, 2005; Suzuki, 2006). Evidence has been reported suggesting that CaCC(s) in intestinal epithelial cells provide an important route for Cl^- and fluid secretion in secretory diarrheas caused by certain drugs (antiretrovirals, chemotherapeutics) and viruses (Morris et al., 1999, Barrett and Keely, 2000; Kidd and Thorn, 2000; Takahashi et al., 2000; Gyömörey et al., 2001; Rufo et al., 2004; Schultheiss et al., 2005, 2006; Thiagarajah and Verkman, 2005; Farthing, 2006; Lorrot and Vasseur, 2007). Smooth-muscle CaCCs have been implicated in the pathophysiology of asthma (Bolton, 2006). Airway CaCCs are found in some model systems to be up-regulated in cystic fibrosis (Tarran et al., 2002), providing an alternative chloride conductance to compensate for missing or defective CFTR.

A significant limitation in studying CaCCs has been the lack of potent or selective inhibitors. Available compounds, including fenamates, anthracene-9-carboxylic acid, indanyloxyacetic acid, ethacrynic acid, and tamoxifen have low potency and inhibit multiple types of Cl^- channels and transporters and in some cases cause activation of BK_{Ca} K^+ channels (Hartzell et al., 2005a). Small-molecule CaCC inhibitors are predicted to be of potential utility in the therapy of certain secretory diarrheas and of excess mucus secretion in asthma and cystic fibrosis (Morris et al., 1999; Rufo et al., 2004; Barnes, 2005; Cuthbert, 2006; Hegab et al., 2007).

The purpose of this study was to identify small-molecule inhibitors of a human intestinal CaCC that target the channel itself or site(s) distal to calcium elevation. Because the molecular identity of intestinal epithelial CaCC(s) is not known, we developed a phenotype-based screening assay using a human intestinal epithelial cell line (HT-29) that grew

This work was supported by grants DK72517, HL73854, EB00415, EY13574, DK35124, and DK43840 from the National Institutes of Health, and Drug Discovery and Research Development Program grants from the Cystic Fibrosis Foundation.
W.N. and A.M. contributed equally to this work.
Article, publication date, and citation information can be found at http://molpharm.aspetjournals.org.
doi:10.1124/mol.107.043208.

ABBREVIATIONS: CFTR, cystic fibrosis transmembrane conductance regulator; CaCC, calcium-activated Cl^- channel; YFP, yellow fluorescent protein; DMEM, Dulbecco's modified Eagle's medium; PBS, phosphate-buffered saline; DMSO, dimethyl sulfoxide; NMDG, *N*-methyl-D-glucamine chloride; CaMKII, calcium-calmodulin protein kinase 2.

well after lentiviral expression of a yellow fluorescent protein (YFP)-type halide sensor (YFP-H148Q/I152L; Jayaraman et al., 2000). As diagrammed in Fig. 1A, the cell-based assay involved measurement of iodide influx in a monolayer of YFP-expressing HT-29 cells in response to a combination of calcium-elevating agonists. A combination of agonists was used to prevent or at least minimize the identification of compounds that target site(s) proximal to cell calcium elevation. CaCC function was quantified from iodide influx as measured from the kinetics of YFP fluorescence quenching after extracellular iodide addition. YFP-expressing epithelial cells have been used in our lab in similar screens to identify small-molecule activators and inhibitors of wild-type and mutant CFTRs (Ma et al., 2002a,b; Yang et al., 2003; Muanprasat et al., 2004; Pedemonte et al. 2005). Compounds with apparent CaCC inhibition activity were prioritized, resynthesized, analyzed for mechanism of action, and subject to structure-activity analysis.

Materials and Methods

Cell Culture and Infection

HT-29 cells were obtained from the American Type Culture Collection (Manassas, VA) and grown in DMEM supplemented with 10% fetal bovine serum (FBS), 100 units/ml penicillin and 100 μg/ml streptomycin. T84 cells (American Type Culture Collection) were maintained in DMEM/Ham's F-12 (1:1) medium containing 10% FBS, 100 units/ml penicillin, and 100 μg/ml streptomycin. Fisher rat thyroid (FRT) cells expressing human CFTR and YFP-H148Q/I152L were generated as described previously (Ma et al., 2002a), and grown in Ham's F-12-modified Coon's medium supplemented with 10% FBS, 2 mM glutamine, 100 units/ml penicillin, and 100 μg/ml streptomycin. All cells were grown at 37°C in 5% CO_2/95% air.

For infection of HT-29 cells with lentivirus encoding YFP-H148Q/I152L, cells were cultured in 90-mm diameter plates in McCoy's 5a medium supplemented with 1.5 mM L-glutamine, 10% FBS, and 2.2 g/l sodium bicarbonate. Cells were cultured until ~80% confluence. Cells were washed three times with PBS, and then 1 ml of a high-titer lentiviral supernatant was added to each well in the presence of 8 μg/ml Polybrene. Cells were incubated at 37°C in 5% CO_2/95% air for 6 h, and medium was then replaced with the regular DMEM growth medium described above. YFP expression was detected in >90% of cells 48 h after infection.

Compounds

Compounds for primary screening were purchased from ChemDiv (San Diego, CA). The compound collection contained 50,000 diverse, drug-like compounds with >90% of compounds in the molecular size range 200 to 450 Da. Compounds for the secondary screening were purchased from ChemDiv and Asinex. Compounds were prepared in 96-well plates (Costar; Corning Life Sciences, Acton, MA) as 10 mM solutions in dimethyl sulfoxide (DMSO). For the primary screen, compounds were tested in groups of four compounds per well.

Screening Procedures

Screening was done using a customized screening system (Beckman-Coulter, Inc., Fullerton, CA) consisting of the SAGIAN Core system integrated with SAMI software, and equipped with an ORCA arm for labware transport, a 96-channel head Biomek FX, CO_2 incubator, plate washer, bar code reader, delidding station, and two FLUOstar Optima fluorescence plate readers (BMG Labtechnologies, Durham, NC), each equipped with syringe pumps and custom excitation/emission filters (500/544 nm; Chroma, Brattleboro, VT). HT-29 cells expressing YFP-H148Q/I152L were plated in 96-well plates at 70% confluence. Plates were incubated overnight at 37°C, 5% CO_2, and then the growth medium was replaced with fresh growth medium. Cells were incubated further until 95% confluence (12–18 h), washed three times with PBS, and incubated with the test compounds at 32.5 μM final concentration for 5 min in PBS, in a final volume of 60 μl/well. YFP fluorescence was measured for 1 s before and 30 s after addition of a PBS-iodide solution (PBS with 100 mM chloride replaced by iodide) containing carbachol and ATP (100 μM each). Each 96-well plate contained "positive" controls (DMSO vehicle without agonists or test compounds) and "negative" controls (DMSO vehicle with agonists but without test compounds). In some experiments, solutions included (individually or in combination): carbachol, ATP, or histamine (at 50, 100, 150, or 200 μM), calcimycin (10 μM), thapsigargin (2 μM), and $CFTR_{inh}$-172 (20 μM). All chemicals were purchased from Sigma-Aldrich (St. Louis, MO). For experiments with thapsigargin or calcimycin, cells in 96-well plates at 100% confluence were washed three times with PBS, incubated with test compounds at 32.5 μM for 5 min in PBS in a final volume of 60 μl/well, and then incubated with 2 μM thapsigargin for 7 min or 10 μM calcimycin for 3 min before assay of iodide influx. Iodide influx ($d[I^-]/dt$ at $t = 0$) was computed from fluorescence time course data by single exponential regression, as described previously (Ma et al., 2002a). Percentage inhibition was computed as: percentage inhibition = $100 \times (\text{Slope}_{\text{negative control}} - \text{Slope}_{\text{test compound}})/(\text{Slope}_{\text{negative control}} - \text{Slope}_{\text{positive control}})$.

CFTR Functional Assay

As described previously (Ma et al., 2002a), FRT cells expressing human wild-type CFTR and YFP-H148Q/I152L at 100% confluence were washed three times with PBS, leaving 60 μl. CFTR was activated by a cocktail containing forskolin (20 μM), genistein (50 μM) and 3-isobutyl-1-methylxanthine (100 μM). Iodide influx was measured at 10 min after addition of test compounds by measuring YFP fluorescence for 2 s before and 20 s after addition of 165 μl of PBS-iodide.

Synthesis Procedures

$CaCC_{inh}$-A01. For synthesis of 6-*t*-butyl-2-(furan-2-carboxamido)-4,5,6,7-tetrahydrobenzo[*b*] thiophene-3-carboxylic acid **1**, a mixture of 4-(*t*-butyl) cyclohexanone (0.154 g, 1.00 mmol), methyl-2-cyanoacetate (0.109 g, 1.1 mmol), morpholine (0.104 g, 1.2 mmol), and ele-

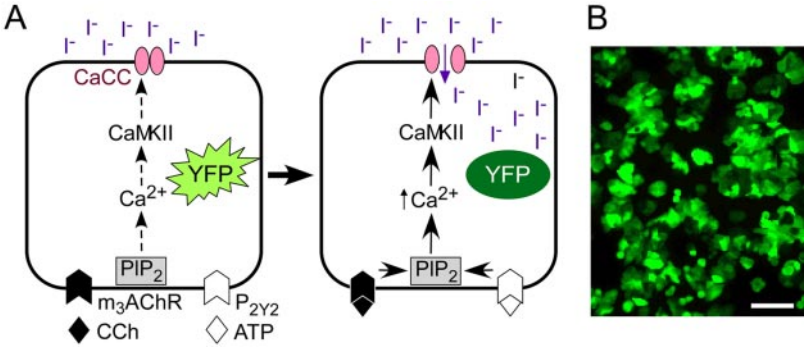

Fig. 1. Assay for CaCC inhibitor screening. A, principle of cell-based, fluorescence high-throughput screening assay. CaCC-facilitated iodide influx is measured from the kinetics of decreasing YFP-H148Q/I152L fluorescence in response to iodide addition to the extracellular solution. CaCC is activated by a mixture of calcium-elevating agonists. CCh, carbachol; m_3AChR, carbachol receptor; P_{2Y2}, purinergic receptor. B, fluorescence micrograph of lentivirus-infected HT-29 cells stably expressing the YFP iodide sensor.

mental sulfur (0.048 g, 1.5 mmol) in methanol (5 ml) were reacted for 10 min at 120°C using a Biotage microwave reactor. Purification by flash chromatography afforded **1** (0.242 g, 0.91 mmol) in 91% yield (Gewald and Hofmann, 1969; Sridhar et al., 2007). Acylation of the amine with furfuryl chloride (0.186 mg, 0.70 mmol) gave compound **2** in 87% yield. Ester hydrolysis of **2** (0.179 g, 0.500 mmol) was accomplished with NaOH in methanol, giving *t*-butylbenzothiophene **3** ($CaCC_{inh}$-A1). $CaCC_{inh}$-A01was purified by column chromatography (160 mg, 91% yield). ^{1}H NMR (400 MHz, $CDCl_3$): δ 12.88 (s, 1H),7.59 (s, 1H), 7.30 (d, J = 3.2 Hz, 1H), 6.59 (dd, J = 7.6 Hz and 2.0 Hz, 1H), 3.18 (d, 2H), 2.72 (m, 2H), 2.43 (t, 1H), 2.05 (m, 1H), 1.51 (m, 1H), 1.35 (m, 1H), 0.95 (s, 9H); ^{13}C NMR ($CDCl_3$): δ 179.2, 170.6, 154.8, 149.1, 146.8, 145.4, 131.8, 128.3, 116.6, 112.9, 94.5, 45.1, 32.6, 27.4, 26.0, 24.5; LC-MS: *m/z* 348.16 $[M+H]^+$ (Nova-Pak C_{18} column, 99%, 200–400 nm).

$CaCC_{inh}$-B01. The synthesis of 2-hydroxy-4-(4-*p*-tolylthiazol-2-ylaminobenzoic acid **4** began with the synthesis of thiourea **5**. Reaction of thiophosgene (2.7 g, 23.890 mmol) with 4-amino-2-hydroxybenzoic acid **2** (3.06 g, 20 mol) in aqueous HCl (41 ml) gave thioisocyanate **4** by crystallization in 83% yield (Seligman et al., 1953). Treatment of thioisocyanate **4** with ammonium hydroxide gave thiourea **5** in 84% yield. Thiazole cyclization of thiourea **5** (0.300 g, 1.415 mmol) with 2-bromo-1-p-tolylethanone (0.298 g, 1.415 mmol) in EtOH (15 ml) gave aminothiazole **6**. The aminothiazole was purified by column chromatography to give $CaCC_{inh}$-B01 (406 mg, 88% yield). ^{1}H NMR (400 MHz, $CDCl_3$): δ 10.67 (s, 1H), 7.80 (d, J = 8.0 Hz, 2H), 7.71 (d, J = 8.1 Hz, 1H), 7.58 (d, J = 2.0 Hz, 1H), 7.36 (s, 1H), 7.25 (d, J = 8.0, 2H), 7.04 (dd, J = 8.1 Hz and 2.0 Hz, 1H), 2.49 (s, 1H), 2.31 (s, 3H); ^{13}C NMR ($CDCl_3$): δ 171.7, 162.7, 162.0, 150.3, 147.2, 137.2, 131.7, 131.3, 129.3, 125.6, 108.5, 105.4, 103.6, 103.1, 20.8; LC-MS: *m/z* 327.11 $[M+H]^+$ (Nova-Pak C_{18} column, 97%, 200–400 nm).

Short-Circuit Current Measurements

T84 cells were seeded at a density of 10^5 cells/cm^2 on permeable supports (Snapwell; 1.12 cm^2 surface area) and grown until confluent. Supports containing confluent cell monolayers were mounted in Snapwell inserts. Cells were bathed for a 30-min stabilization period in HCO_3^--buffered solution containing 120 mM NaCl, 5 mM KCl, 1 mM $MgCl_2$, 1 mM $CaCl_2$, 10 mM D-glucose, 5 mM HEPES, and 25 mM $NaHCO_3$, pH 7.4, aerated with 95% O_2/5% CO_2 at 37°C. Monolayers were voltage-clamped at 0 mV (EVC4000 MultiChannel V/I Clamp; World Precision Instruments, Sarasota, FL), and short-circuit current (Isc) was recorded continuously with agonists/inhibitors added at specified times.

Patch-Clamp

Whole-cell recordings were done on HT-29 cells at room temperature. The pipette solution contained 30 mM CsCl, 100 mM Cs-aspartate, 1 mM $MgCl_2$, 0.5 mM EGTA, 2 mM Tris-ATP, and 10 mM HEPES, pH 7.2 with CsOH, and the bath solution contained 140 *N*-methyl-D-glucamine chloride (NMDG-Cl), 1 mM $CaCl_2$, 1 mM $MgCl_2$, 10 mM glucose, and 10 mM HEPES, pH 7.2. In one set of studies, symmetric NMDG-Cl solutions contained 140 mM NMDG-Cl, 1 mM $MgCl_2$, 0.5 mM EGTA, 2 mM Tris-ATP, and 10 mM HEPES, pH 7.2. Pipettes were pulled from borosilicate glass and had resistances of 3 to 5 MΩ after fire polishing. Seal resistances were typically between 3 to 10 GΩ. After establishing the whole-cell configuration, CaCCs were activated by 1 μM ionomycin. Whole-cell currents were elicited by applying hyperpolarizing and depolarizing voltage pulses from a holding potential of 0 mV to potentials between −120 mV and +120 mV in steps of 20 mV. Currents were filtered at 5 kHz, and digitized and analyzed using an AxoScope 10.0 system with Digidata 1440A converter (Molecular Devices, Sunnyvale, CA). Mean currents were expressed as current densities (picoampere per picofarad).

$[Ca^{2+}]_i$ Measurements

$[Ca^{2+}]_i$ was measured in confluent monolayers of HT-29 cells after loading with Fura-2 (2 μM Fura-2-AM, 30 min, 37°C). Labeled cells were mounted in a perfusion chamber on the stage of an inverted epifluorescence microscope. Cells were superfused with 140 mM NaCl, 5 mM KCl, 1 mM $MgCl_2$, 1 mM $CaCl_2$, 10 mM D-glucose, and 10 mM HEPES, pH 7.4, initially without and then with ATP/carbachol. Test compounds were present in some experiments for 10 min before agonist addition. Fura-2 fluorescence was recorded at excitation wavelengths of 340 nm and 380 nm using standard procedures.

Immunoblotting

Calcium/calmodulin-dependent protein kinase II (CaMKII) was activated by 2-min treatment of HT-29 cells with ATP/carbachol (each 100 μM). Cells were then lysed with cell lysis buffer (20 mM Tris-HCl, pH 7.4, 1% Triton X-100, 150 mM NaCl, 2 mM EDTA, 50 mM α-glycerol phosphate, 1 mM Na_3VO_4, 1 mM dithiothreitol, and protease inhibitor mixture (Roche Applied Science). Cell debris was removed by centrifugation, and proteins in the supernatant were resolved by SDS-polyacrylamide gel electrophoresis and immunoblotted using standard procedures (transfer to polyvinylidene difluoride membrane, 1 h blocking in 5% nonfat dry milk, primary/secondary antibody incubations, enhanced chemiluminescence detection). Rabbit polyclonal antibodies for anti-phospho-CaMKII (Thr286) and β-actin were purchased from Cell Signaling Technology (Danvers, MA).

Results

High-Throughput Screening Assay Development and Validation. As diagrammed in Fig. 1A, our assay used a human intestinal cell line (HT-29) having robust CaCC activity. In the presence of calcium-elevating agonist(s), extracellular iodide addition results in CaCC-facilitated iodide influx, which is detected by fluorescence quenching of a cytoplasmic YFP-based halide sensor (YFP-H148Q/I152L). After lentiviral infection, HT-29 cells stably expressing YFP-H148Q/I152L were brightly fluorescent, with nearly all cells showing fluorescence (Fig. 1B). Alternative human intestinal epithelial cells lines, including T84 and Caco-2 cells, were found to be inadequate for screening because of slow growth, lack of growth to confluent monolayers, poor YFP expression, and/or weak CaCC activity.

Several CaCC agonists were assayed to establish the cellular model for CaCC inhibitor screening. Histamine (100 μM), calcimycin (10 μM), ATP (100 μM), carbachol (100 μM), and forskolin (10 μM) were tested individually (Fig. 2A) and in combinations (Fig. 2B). The CFTR inhibitor $CFTR_{inh}$-172 (20 μM) was also tested. Of the agonists tested individually, carbachol and ATP produced the strongest responses as seen from the slopes of the fluorescence decrease after extracellular iodide addition. In combination, carbachol and ATP produced as large a response as seen for any of the combinations. Increased iodide influx was not found after forskolin addition, and $CFTR_{inh}$-172 did not inhibit iodide influx in response to calcium agonists, indicating that the cell clone used in our assay expressed little or no functional CFTR.

A combination of carbachol and ATP, each at high concentration, was selected for compound screening, reasoning that any inhibitors should act beyond the receptor binding step. Iodide influx measurements were done to establish agonist concentrations and addition times. Concentration dependence studies for carbachol (Fig. 2C) and ATP (not shown) indicated maximal responses at 100 μM. Figure 2D shows reduced iodide influx as a function of time between addition

of 100 μM carbachol/ATP and extracellular iodide, which is consequence of the transient elevation in cytoplasmic calcium produced by these agonists. The greatest iodide influx was found when agonists were added at ~10 s before iodide, although the influx was not much greater than when agonists were added at the time of iodide addition. For high-throughput screening, to simplify assay conditions, agonists (carbachol and ATP, each 100 μM) were added together with iodide.

CaCC Inhibitor Identification by High-Throughput Screening. To characterize the assay as used for high-throughput screening, iodide influx was measured in the YFP-expressing HT-29 cells in a 96-well format using an automated workstation capable of assaying more than 10,000 compounds overnight. Figure 3A, left, shows representative YFP fluorescence kinetics measured in single wells of 96-well plates. Each curve consisted of recording of baseline fluorescence for 1 s, followed by 30 s of continuous recording of fluorescence after rapid addition of a solution containing iodide and the CaCC agonist combination (carbachol and ATP, each 100 μM). After a small solution addition artifact, there was little decrease in fluorescence in the absence of activators, compared with a robust reduction in fluorescence with agonists. Figure 3A (right) shows frequency histograms of iodide influx rates, $d[I^-]/dt$, in individual wells for "positive" (no agonists, equivalent to 100% inhibition) and "negative" (with agonists, 0% inhibition) controls. The computed Z′-factor (Verkman, 2004) for the assay was very good, 0.74, indicating adequacy of a single compound screening to identify putative CaCC inhibitors. The presence of DMSO (from compound addition) did not affect assay quality.

Based on initial small-scale screenings at different compound concentrations, which showed a low "hit" rate for discovery of active compounds, we screened 50,000 compounds at a concentration 32.5 μM. Figure 3B, left, shows examples of data from single wells for compounds with "strong," "weak," and no inhibition activity. Figure 3B, right, summarizes percentage inhibition data as a frequency histogram. Of 50,000 small molecules screened (in groups of four), 300 compound groups had CaCC inhibitory activity as defined arbitrarily by a 70% cutoff (vertical dashed line). Retesting of these 300 compound groups indicated a false-positive rate of ~40%.

Further analysis was done on 15 compound groups that produced greatest inhibition when retested at 10 and 30 μM concentrations. The compound responsible for activity in each group was determined by testing of individual compounds. In each case, a single active compound was identified in the groups of four. Figure 4A shows structures of the most active of six classes of putative CaCC inhibitors (classes A–F) identified by single compound testing; in some cases, particularly for classes A and B, similar structures were seen several times. These structures are unrelated to all known Cl^- channel inhibitors. Percentage inhibition of these compounds at 30 μM was in the range 60 to >90%. Based on multiple criteria, including potency, water solubility, drug-like properties, identification of active analogs, chemical stability, and CaCC targeting, we focused attention on compounds of classes A and B. As shown below, the class E compound did not inhibit iodide influx in response to thapsigargin, suggesting that its target is proximal in the calcium signaling pathway, and thus not of interest here. The class D compound was determined to have poor stability in aqueous solutions, probably because of retro-Diels-Alder reaction.

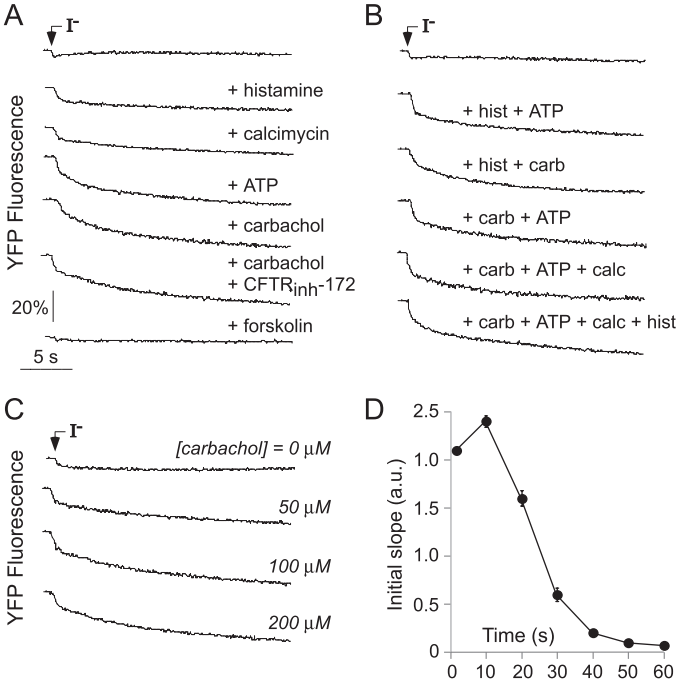

Fig. 2. Functional characterization of YFP-expressing HT-29 cells. Time course of YFP fluorescence after extracellular iodide addition. As indicated, solutions contained histamine (100 μM), calcimycin (10 μM), ATP (100 μM), carbachol (100 μM), carbachol (100 μM) + $CFTR_{inh}$-172 (20 μM), or forskolin (20 μM), individually (A), and in various combinations (at same concentrations) (B). The scale-bar on the *y*-axis indicates the percentage reduction in fluorescence relative to baseline fluorescence (before iodide addition). C, carbachol concentration-response study. D, initial negative fluorescence curve slope (after extracellular iodide addition) as a function of time after carbachol/ATP (each 100 μM) addition and extracellular iodide addition.

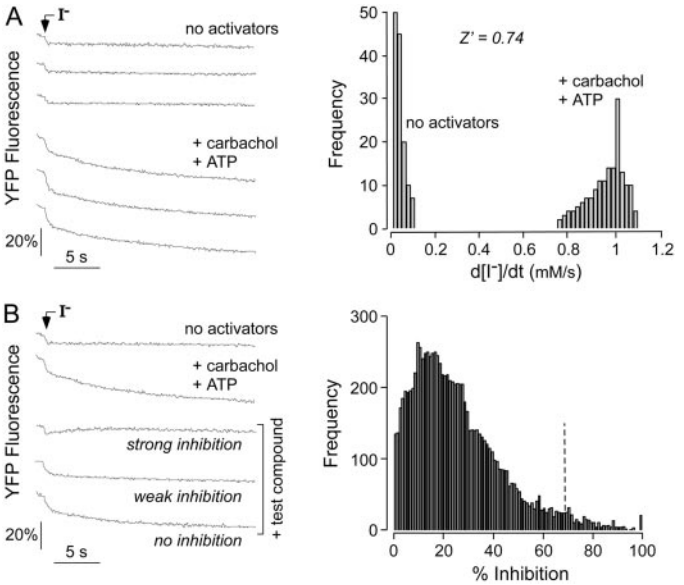

Fig. 3. CaCC inhibitor screening. A, screen validation. Left, time course of YFP fluorescence in HT-29 cells after iodide addition in the absence or presence of carbachol (100 μM) and ATP (100 μM). Right, histogram distribution of iodide influx rates ($d[I^-]/dt$) determined from initial fluorescence slopes. B, left, examples of fluorescence data for individual compounds in the primary screen. Right, histogram distribution of percentage inhibition from primary compound screening. Dashed vertical line denotes selection criteria for further evaluation.

Class F compounds were excluded from further study because of their small size and relatively low potency.

Synthesis and Characterization of Class A and B Compounds. Before further analysis of their biological activities and mechanisms of action, we synthesized the class A and B compounds to high purity and verified their structures and chemical stability in aqueous solutions. The synthesis of CaCC$_{inh}$-A01 was accomplished in three steps (Fig. 4B, top), involving Knovenagle condensation of methyl cyanoacetate with *t*-butylcyclohexanone followed by cyclization on elemental sulfur. Purification by flash chromatography produced the 2-aminothiophene Gewald product. Acylation of the aminothiophene gave the *N*-acyl methyl ester **2** in good yield. Ester **2** was hydrolyzed with NaOH to give CaCC$_{inh}$-A01 **3**, which was purified by chromatography and recrystallization. Synthesis of CaCC$_{inh}$-B01 also involved three steps (Fig. 4B, bottom). Reaction of 4-amino-2-hydroxybenzoic acid with thiophosgene in HCl gave isothiocyanate **4** in good yield. Treatment of **4** with ammonium hydroxide gave thiourea **5,** which was then reacted with 2-bromo-1-*p*-tolylethanone to give CaCC$_{inh}$-B01 **6**.

CaCC$_{inh}$-A01 and CaCC$_{inh}$-B01 were confirmed by ^{1}H-NMR, ^{13}C-NMR and mass spectrometry (analytical data provided under *Materials and Methods*). The aqueous solubility of CaCC$_{inh}$-A01 and CaCC$_{inh}$-B01 in PBS was >500 μM, as measured by optical absorbance of a saturated solution after appropriate dilution. The high aqueous solubility of CaCC$_{inh}$-A01 and CaCC$_{inh}$-B01 is a consequence of their polarity and negative charge at physiological pH. By liquid chromatogra-

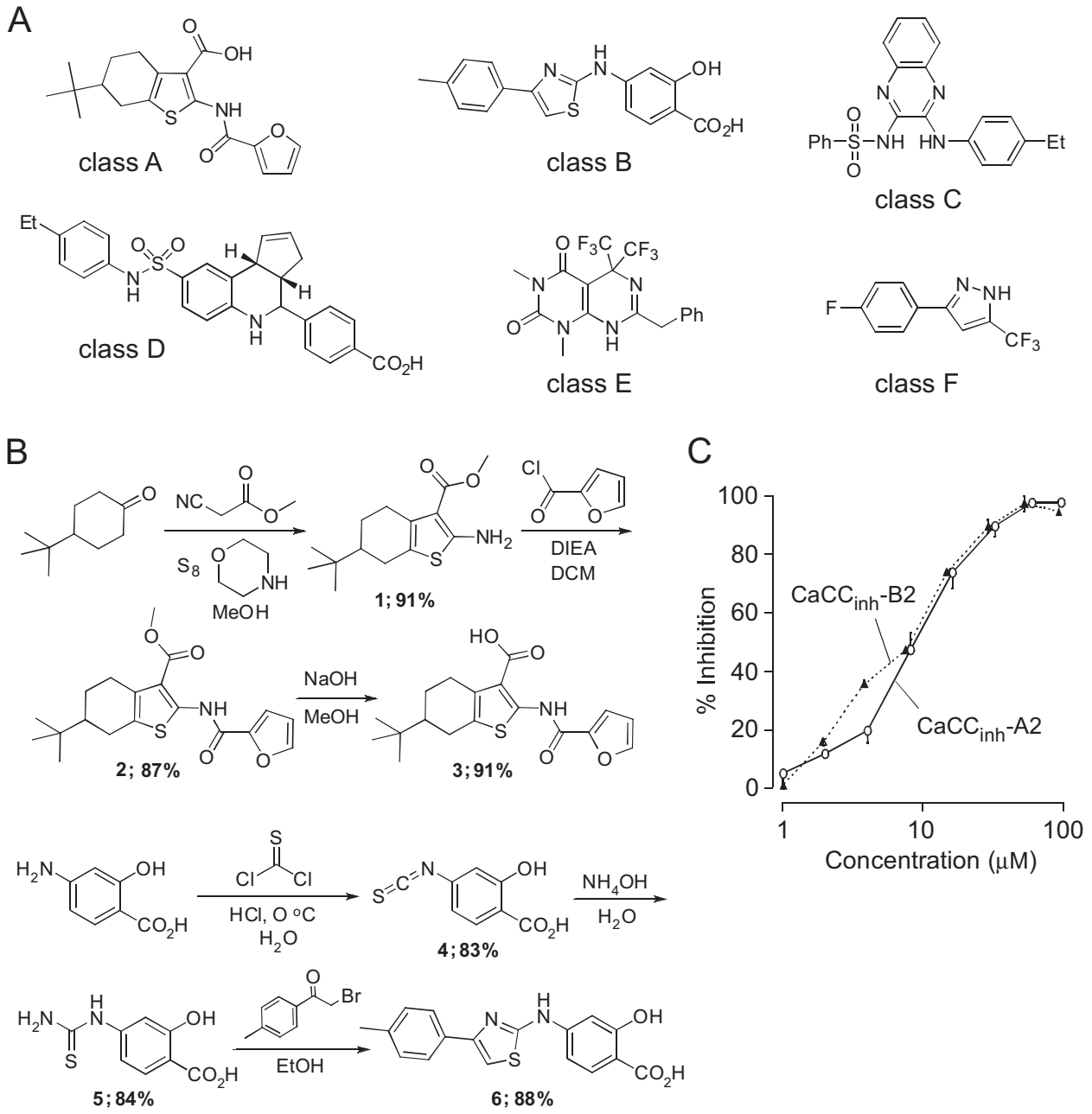

Fig. 4. Structures and synthesis of putative CaCC inhibitors. A, structures of compounds of classes A–F identified from the primary screen. B, synthesis of CaCC$_{inh}$-A01 and CaCC$_{inh}$-B01. See *Materials and Methods* for details. C, concentration-inhibition data for CaCC$_{inh}$-A01 and CaCC$_{inh}$-B01 determined by plate reader fluorescence assay.

phy, purity was 97% and 99% for $CaCC_{inh}$-A01 and $CaCC_{inh}$-B01, respectively.

Testing of the purified compounds using the fluorescence plate-reader assay verified their activities, with IC_{50} values ~10 μM (Fig. 4C). These apparent IC_{50} values are only semiquantitative because of the multistep nature of the screening assay and because of the ~3-fold compound dilution at the time of iodide addition during the assay. Accurate IC_{50} values were determined by electrophysiological assays (see below).

Target Identification. Several targets are possible based on the screening strategy in Fig. 1A, including ligand-receptor binding, calcium elevation, calcium-calmodulin (CaMKII) signaling, and the CaCC itself. To distinguish between pre- and postcalcium signaling targets, compounds of each class were tested after stimulation of HT-29 cells by thapsigargin, which produces calcium elevation without ligand-receptor binding or phosphoinositide signaling. Figure 5A shows that each of the compounds inhibited iodide influx after thapsigargin, except for the class E compound, whose target is thus

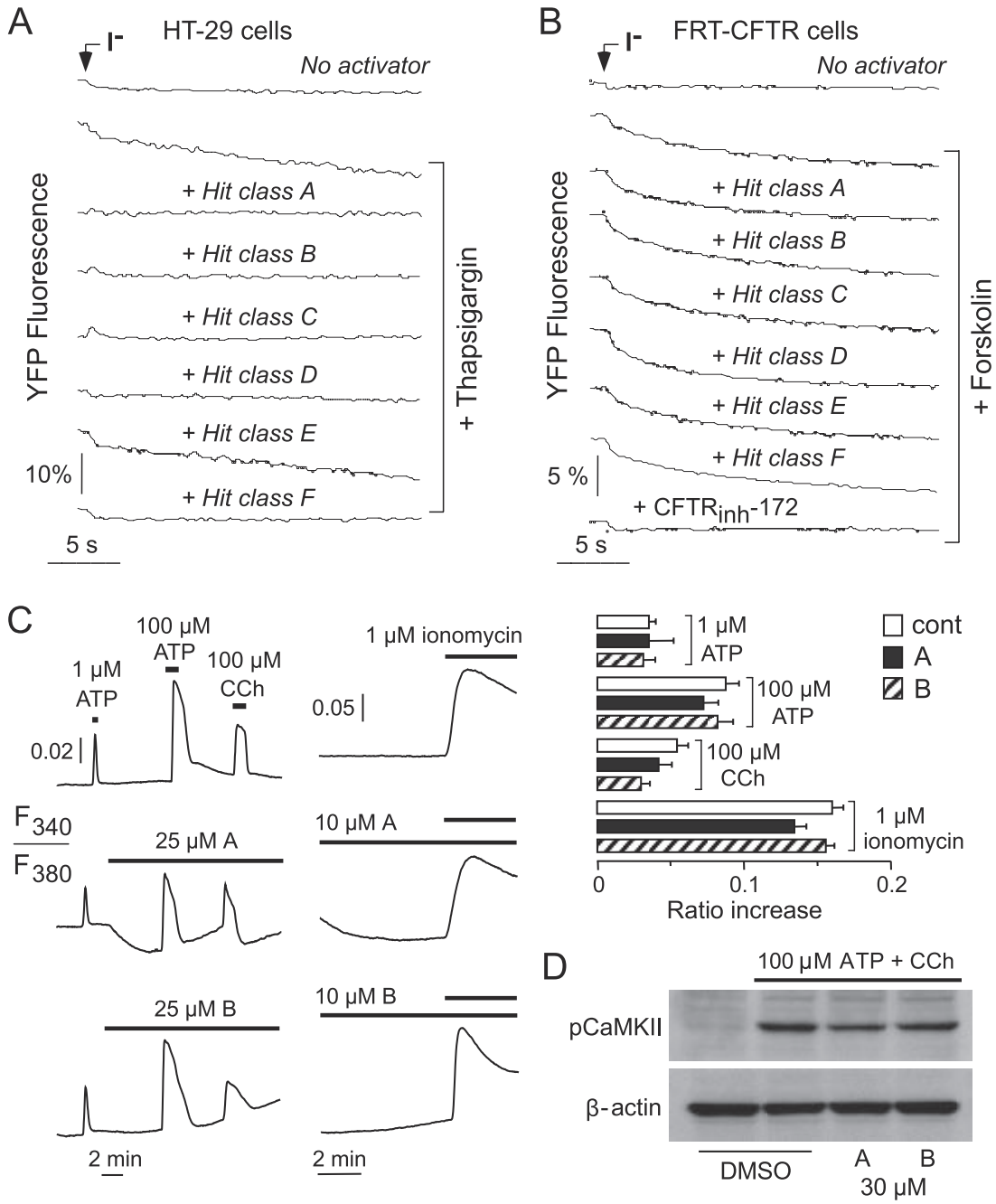

Fig. 5. Target dissection studies. A, time course of YFP fluorescence in HT-29 cells after iodide addition in the absence or presence of thapsigargin in cells pretreated with 30 μM concentrations of the indicated compounds. B, YFP fluorescence in FRT cells expressing human wild-type CFTR after iodide addition in cells pretreated with 30 μM concentrations of the indicated compounds. $CFTR_{inh}$-172 (20 μM) was present where indicated. C, calcium signaling measured by fura-2 fluorescence in response to indicated agonists and test compounds. A, $CaCC_{inh}$-A01. B, $CaCC_{inh}$-B01. Representative data shown on the left, with averaged data on the right (SE, $n = 3–4$). Differences not significant. D, ATP/carbachol-induced CaMKII phosphorylation determined by immunoblot analysis (representative of three separate experiments).

likely upstream of calcium signaling. Experiments were also done to rule out compound effects on CFTR, because CFTR is a major intestinal chloride channel, and there is evidence for cross-talk between cAMP and calcium signaling in intestinal cell chloride secretion (Chao et al., 1994; Takahashi et al., 2000; Schultheiss et al., 2006). Using our well established FRT-CFTR assay, Fig. 5B shows no CFTR inhibition by any of the compounds at 30 μM, with $CFTR_{inh}$-172 inhibition shown as positive control.

Measurements of cytoplasmic calcium were done to investigate whether $CaCC_{inh}$-A01 and $CaCC_{inh}$-B01 interfered with agonist-induced calcium signaling in HT-29 cells. Figure 5C shows $[Ca^{2+}]_i$ elevations in response to 1 μM ATP, 100 μM ATP, and 100 μM carbachol (left), or 1 μM ionomycin (middle). Pretreatment with $CaCC_{inh}$-A01 or $CaCC_{inh}$-B01 at high concentration before agonist addition did not significantly reduce the ATP- or carbachol-induced $[Ca^{2+}]_i$ elevations (right).

Regulation of CaCC activation by CaMKII occurs in a cell type-dependent manner (Hartzell et al., 2005a). CaMKII has been reported to regulate calcium-activated chloride currents in HT-29 and T84 cells (Worrell and Frizzell, 1991; Morris and Frizzell, 1993; Chan et al., 1994; Braun and Schulman, 1995). To determine whether the CaCC inhibitors interfered with ATP/carbachol-induced CaMKII activation, CaMKII phosphorylation in HT-29 cells was measured by immunoblot analysis. CaMKII was activated by a 2 min incubation with 100 μM ATP/carbachol. Figure 5D shows strong pCaMKII immunoreactivity after agonist treatment. Pretreatment with 30 μM $CaCC_{inh}$-A01 or $CaCC_{inh}$-B01 did not significantly affect agonist-induced CaMKII phosphorylation. β-Actin is shown as a loading control.

Whole-cell patch-clamp was done to investigate the inhibition of calcium-dependent chloride current in HT-29 cells by $CaCC_{inh}$-A01 and $CaCC_{inh}$-B01. Measurements were carried out under K^+-free conditions (Cs^+ in pipette) to ensure that chloride currents were being measured. Treatment with 1 μM ionomycin produced large currents of 28 ± 3 pA/pF (V_m +100 mV) in NMDG-Cl solutions, with an outwardly rectifying current-voltage relationship (Fig. 6, A and B). Ionomycin-stimulated currents were measured when the current was maximally activated at a V_m of −40 mV and current density data were analyzed at V_m of +100 mV. As summarized in Fig. 6C, calcium-dependent chloride current was reduced by 38 ± 14, 66 ± 10, and 91 ± 1% by 0.1, 1, and 10 μM $CaCC_{inh}$-A01, respectively, and by 11 ± 7, 34 ± 12, and 77 ± 4% by 0.1, 1, and 10 μM $CaCC_{inh}$-B01. As a control to exclude interference by transient receptor potential and nonselective cation channels, ionomycin-induced chloride currents were also recorded in the whole-cell configuration using symmetric NMDG-Cl solutions (Fig. 6D). As predicted, pretreatment with $CaCC_{inh}$-A01 and $CaCC_{inh}$-B01 reduced ionomycin-induced currents.

Chloride secretion was also measured in T84 cells to investigate whether the CaCC inhibitors identified from screening of HT-29 cells also inhibit the CaCC in a different human intestinal cell line. ATP/carbachol were used to induce calcium-dependent chloride secretion in well differentiated T84 cell monolayers. The increase in short-circuit current in response to carbachol (without inhibitors added) was similar in all experiments (Fig. 7A). Subsequent application of 100 μM ATP ~30 min later produced a large response (top curve), which was reduced in the presence of inhibitors (lower four curves). Carbachol and ATP-induced short-circuit currents

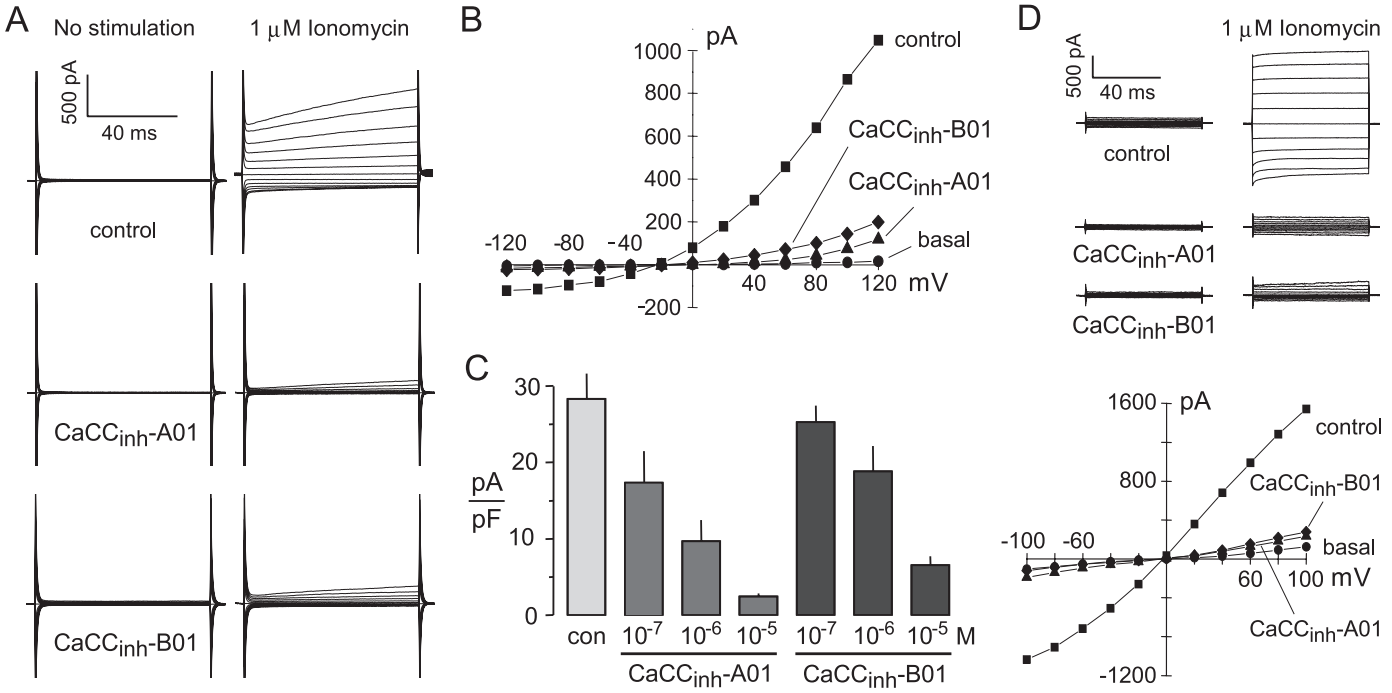

Fig. 6. Patch-clamp analysis of CaCC inhibitors. CaCC channel activity in the whole-cell configuration was measured HT-29 cells. A, ionomycin-induced currents in asymmetrical solutions in the absence or presence of $CaCC_{inh}$-A01 or $CaCC_{inh}$-B01 (each 10 μM) recorded at a holding potential at 0 mV, and pulsing to voltages between ± 120 mV in steps of 20 mV (see *Materials and Methods*). B, current/voltage (I/V) plot of mean currents at the end of each voltage pulse from experiments as in A. C, summary of current density data measured at V_m of + 100 mV (S.E., n = 6–8). D, top, ionomycin-induced chloride currents in the whole-cell configuration with symmetrical NMDG-Cl solutions. Bottom, current/voltage plot of mean currents at the end of each voltage pulse.

are summarized in Fig. 7B. ATP-induced short-circuit currents were reduced by 38 ± 7 and 78 ± 3% at 10 and 30 μM $CaCC_{inh}$-A01, respectively, and by 29 ± 11 and 64 ± 3% by 10 and 30 μM $CaCC_{inh}$-B01, respectively.

Structure-Activity Analysis. An important characteristic of small molecules for drug development is the existence of many active chemical analogs ("evolvable" SAR) to allow optimization of drug properties. SAR analysis was performed on 936 commercially available aminothiophenes (class A analogs) and 944 aminothazoles (class B analogs). Tables 1 and 2 provide semiquantitative CaCC inhibition data (from plate reader assay) for 18 active aminothiophenes (class A) and 14 active aminothiazoles (class B). Figure 8 summarizes the SAR analysis in terms of the functional groups conferring CaCC inhibition activity based on consideration of data for all analogs tested. An essential moiety for strong activity in both compound classes was the presence of a carboxylic acid functional group, as has been found in most chloride channel inhibitors.

For class A compounds, *t*-butyl at position R_1 conferred the greatest inhibition; inhibition was reduced or lost when R_1 was methyl or H, as with analogs $CaCC_{inh}$-A12-A15 (many inactive methyl analogs not included in Table). Modification of the cyclohexyl ring system to cyclopentyl and cycloheptyl (varying n) indicated greatest activity with six membered rings. Several cycloheptylthiophenes were found to be active but much less potent than the six membered ring analogs. At R_2, hydroxy, methoxy, ethoxy, and substituted phenyl amides

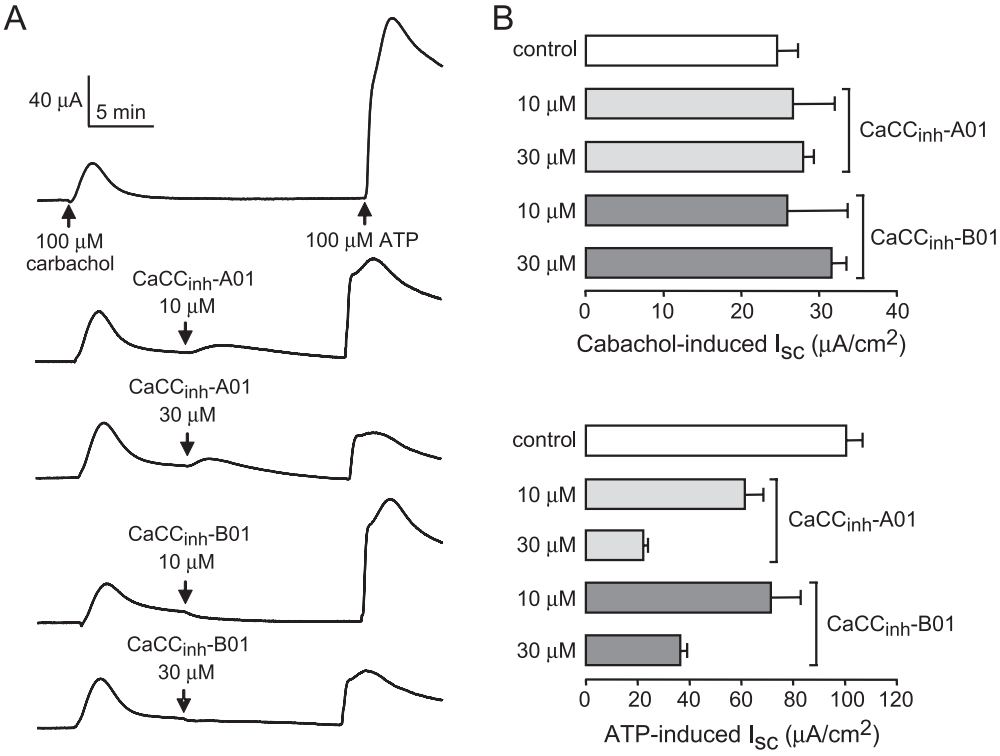

Fig. 7. Inhibition of chloride secretion in T84 cells by short-circuit current analysis. A, After carbachol stimulation, ATP-induced I_{sc} was measured in the absence or presence of inhibitors (representative of three or four separate experiments). B, summary of short-circuit currents induced by carbachol and ATP for experiments as in A (S.E., n = 3–4). (Inhibitors not present for carbachol stimulation).

TABLE 1
Structure-activity of Class A CaCC inhibitors
See Fig. 8 for locations of R1, R2, and R3 and meaning of *n*.

Compound	R1	R2	R3	*n*	Inhibition at 25 μM
					%
$CaCC_{inh}$-A01	*t*-butyl	OH	CO-furanyl	0	100
$CaCC_{inh}$-A02	*t*-butyl	OH	CO-2-methylphenyl	0	95
$CaCC_{inh}$-A03	*t*-butyl	OH	CO-3-chlorophenyl	0	50
$CaCC_{inh}$-A04	*t*-butyl	OH	CO-phenyl	0	85
$CaCC_{inh}$-A05	*t*-butyl	OH	CO-2-chlorophenyl	0	75
$CaCC_{inh}$-A06	*t*-butyl	OEt	$CO\text{-}CH_2CH_2CO_2H$	0	75
$CaCC_{inh}$-A07	*t*-butyl	OEt	$(trans)COCH = CHCO_2H$	0	98
$CaCC_{inh}$-A08	*t*-butyl	OEt	CO-2-carboxycyclohexyl	0	80
$CaCC_{inh}$-A09	*t*-butyl	OMe	$CO\text{-}CH_2CH_2CH_2CO_2H$	0	45
$CaCC_{inh}$-A10	$EtMe_2C$-	OEt	CO-2-carboxycyclohexyl	0	75
$CaCC_{inh}$-A11	*t*-butyl	OMe	$CO\text{-}CH_2CH_2CO_2H$	0	81
$CaCC_{inh}$-A12	H	OH	CO-4-methylphenyl	1	15
$CaCC_{inh}$-A13	H	OH	CO-phenyl	1	27
$CaCC_{inh}$-A14	H	OH	CO-2-chlorophenyl	1	18
$CaCC_{inh}$-A15	H	OH	CO-3-methoxyphenyl	0	20
$CaCC_{inh}$-A16	*t*-butyl	NH-3-MePhCO-	$CH_2CH_2CO_2H$	0	42
$CaCC_{inh}$-A17	H	OH	CO-3-methylphenyl	0	7
$CaCC_{inh}$-A18	*t*-butyl	NH-4-MeOPh CO-	$CH_2CH_2CO_2H$	0	35

Ph, phenyl; Br, bromo; Cl, chloro; F, fluoro; OMe, methoxy; NO_2, nitro.

were tolerated. If R_2 is OH, as in the carboxylic acid, then R_3 can be a substituted phenyl ring or heterocycle as seen in $CaCC_{inh}$-A01-A05, -A15, and -A17. Methyl and ethyl esters were tolerated at R_2 if an alkyl carboxylic acid was present at R_3 as seen in $CaCC_{inh}$-A06-A11. Substituted phenyl amides at R_2 had weak activity as seen in $CaCC_{inh}$-A16 and $CaCC_{inh}$-A18. For R_3, activity was found for substituted phenyl rings, heterocycles, and alkyl carboxylic acids such as 3-carboxypropanamido, *trans*-3-carboxyacrylamido, and 2-carboxycyclohexane-carboxamido, but only when R_2 was OMe, OEt, or NHPh. Of the alkyl substituted carboxylic acids at R_3, the most active analog was the *trans*-3-carboxyacrylamido in $CaCC_{inh}$-A07. CO-phenyl substitutions at R_3 were tolerated in active compounds with the 2-position favored. Electron-donating substituents led to substantially reduced activity. A variety of heterocycles were screened at R_3 with only CO-furfuryl active, The most potent compound was 6-*tert*-butyl-2-(cyclopenta-1,3-dienecarboxamido)-4,5,6,7-tetrahydrobenzo-[*b*]thiophene-3-carboxylic acid ($CaCC_{inh}$-A01).

For class B, at position R_1 methyl substitution at the 4 position of the aromatic ring was present in most active compounds as seen in $CaCC_{inh}$-B01-B06. Additional methyl substitution at the 2 position gave active analogs $CaCC_{inh}$-B07-B09. Inhibition was greatly reduced when the phenyl ring was substituted at the 2 or 3 positions. As with class A, a carboxylic acid functional group was essential for activity, either with an alkyl substitution at R_2 or a phenyl substitution at R_3. Loss of this carboxylic acid functionality reduced activity as seen in $CaCC_{inh}$-B09-B13. At position R_2, most active compounds contained either hydrogen substitution or an acetic acid group. For position R_3, a variety of phenyl substitutions were tolerated, the majority being alkyl or halogen substitution at the 3 and 4 positions. Electron donating substituents produced inactive compounds. The SAR

TABLE 2
Structure-activity of Class B CaCC inhibitors
See Fig. 8 for locations of R1, R2, and R3 and meaning of *n*.

Compound	R1	R2	R3	Inhibition at 25 μM
				%
$CaCC_{inh}$-B01	4-Me	-H	3-Carboxylate-4-hydroxyphenyl	100
$CaCC_{inh}$-B02	4-Me	$-CH_2CO_2H$	3-Chloro-4-methylphenyl	40
$CaCC_{inh}$-B03	4-Me	$-CH_2CO_2H$	3-Bromophenyl	60
$CaCC_{inh}$-B04	4-Me	$-CH_2CO_2H2$,	4-Dichlorophenyl	65
$CaCC_{inh}$-B05	4-Me	$-CH_2CO_2H$	3-Trifluoromethylphenyl	60
$CaCC_{inh}$-B06	2,4-DiMe	-Pr	4-Carboxylatephenyl	100
$CaCC_{inh}$-B07	2, 4-DiMe	$-CH_2CO_2H$	4-Bromophenyl	70
$CaCC_{inh}$-B08	2,4-DiMe	$-CH_2CO_2H$	3-Trifluoromethylphenyl	75
$CaCC_{inh}$-B09	4-PhO	-H	4-Isobutylphenyl	65
$CaCC_{inh}$-B10	3-CF_3	-H	4-Cyclohexylphenyl	55
$CaCC_{inh}$-B11	4-Me	$-CH_2CO_2H$	4-Ethoxyphenyl	65
$CaCC_{inh}$-B12	4-Me	-Ph	CO-3-Methylphenyl	3
$CaCC_{inh}$-B13	4-Me	-H	Ethyl	20
$CaCC_{inh}$-B14	4-MeO	$-CH_2CH_2CO_2H$	4-Methoxyphenyl	18

Ph, phenyl; Br, bromo; Cl, chloro; F, fluoro; OMe, methoxy; NO_2, nitro.

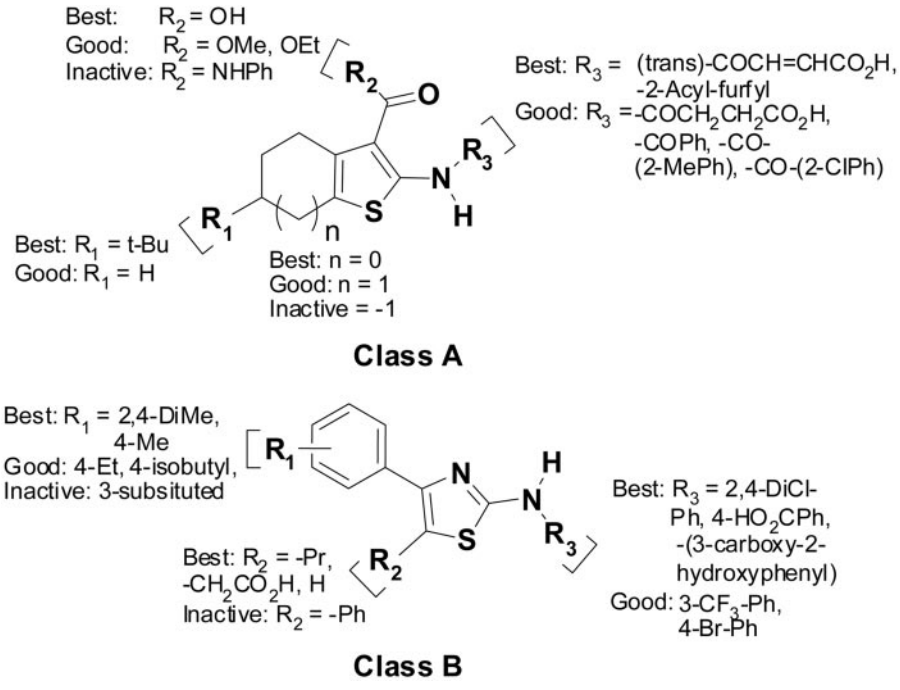

Fig. 8. Structure-activity analysis of CaCC inhibitors. Summary of SAR conclusions for class A and B CaCC inhibitors. See *Structure-Activity Analysis* under *Results*, for explanations.

study thus indicates the existence of many active class A and B CaCC inhibitors having a wide range of potencies.

Discussion

Our phenotype-based small-molecule screen identified novel chemical classes of inhibitors of CaCC conductance, two of which seem to target the CaCC itself rather than upstream signaling mechanisms. The aminothiophenes and aminothazoles did not interfere with agonist-induced cytoplasmic calcium elevation or calmodulin (CaMKII) phosphorylation, and by patch-clamp analysis inhibited CaCC gating. The data here do not distinguish between an external versus internal site of compound action, nor do they provide information about the molecular identity of the intestinal CaCC responsible for the observed chloride conductance, though determination of comparative compound potencies on candidate CaCCs, as mentioned in the Introduction, may offer indirect evidence about CaCC identity. The verified "hit" rate for our small-molecule screen, ~1 per 10,000 compounds tested, is in the range generally found in ion channel inhibitor screens. Therefore, further screening of larger collections of diverse compounds is likely to succeed in identifying new chemical classes of CaCCs.

Our high-throughput screening assay used a kinetic fluorescence measurement of iodide influx in an intestinal epithelial cell line. Iodide is superior to chloride for primary screening because of its transport by channels and not by exchangers or cotransporters, such as AE1 (Cl^-/HCO_3^-) and NKCC ($Na^+/K^+/2Cl^-$), and its substantially greater quenching compared with chloride of available molecular and chemical halide sensors (Verkman and Jayaraman, 2002). Furthermore, of specific relevance to the CaCC screening here, all CaCCs that have been tested show greater iodide versus chloride conductance (Eggermont, 2004; Hartzell et al., 2005). The YFP indicator used for screening, YFP-H148Q/I152L, which is 50% quenched by ~3 mM iodide, was discovered by screening of ~1000 YFP analogs for halide sensitivity (Galietta et al., 2001). YFPs have been applied, in other cell types, for small-molecule screens to identify inhibitors (Ma et al., 2002b; Muanprasat et al., 2004) and activators (Ma et al., 2002a) of wild-type CFTR and for potentiators (Yang et al., 2003) and correctors (Pedemonte et al., 2005) of ΔF508-CFTR, the major CFTR mutation causing cystic fibrosis. We have also used a YFP/iodide screening strategy in a "pathway" screen to identify G-protein coupled receptor antagonists (Yangthara et al., 2007). The cell line used here and the introduction method for stable YFP expression were selected after screening of existing human intestinal epithelial cell lines (T84, HT-29, Caco-2) and transfection methods (plasmids, viruses). Lentiviral introduction of YFP in HT-29 cells produced a cell line suitable for screening that fulfilled the key requirements of efficient growth on plastic, bright YFP fluorescence, strong CaCC chloride conductance, and low basal (CaCC-independent) iodide conductance.

CaCC(s) have been reported previously to be expressed in undifferentiated HT-29 and T84 cells (Worrell and Frizzell, 1991; Morris and Frizzell, 1993; Chan et al., 1994; Arreola et al., 1995; Braun and Schulman, 1995). Our patch-clamp and short-circuit current results are in agreement with these prior data. We found ionomycin-induced calcium-dependent chloride currents in HT-29 cells with typical outwardly rectifying current-voltage relationships (Arreola et al., 1995; Braun and Schulman, 1995; Nilius et al., 1997), as well as ionomycin-induced calcium-dependent chloride current in T84 cells. Chloride currents in both cell types were strongly inhibited by the aminothiophenes and aminothazoles discovered here, suggesting common CaCC(s) in these cell types and indicating little or no inhibitor-insensitive calcium-dependent chloride current.

In summary, we report the development and validation of an efficient screen for identification of inhibitors of intestinal CaCCs, along with the identification and characterization of several classes of active compounds from a screen of 50,000 compounds. These or other compounds identified from similar screens, with follow-on work, may be useful for molecular identification of CaCCs and for therapeutic applications in certain secretory diarrheas and in lung diseases associated with mucus overproduction.

References

Arreola J, Melvin JE, and Begenisich T (1995) Inhibition of Ca^{2+}-dependent Cl^- channels from secretory epithelial cells by low internal pH. *J Membr Biol* **147:**95–104.

Barnes PJ (2005) Emerging targets for COPD therapy. *Curr Drug Targets Inflamm Allergy* **4:**675–683.

Barrett KE, Keely SJ (2000) Chloride secretion by the intestinal epithelium: molecular basis and regulatory aspects. *Annu Rev Physiol* **62:**535–572.

Bolton TB (2006) Calcium events in smooth muscles and their interstitial cells; physiological roles of sparks. *J Physiol* **570:**5–11.

Braun AP and Schulman H (1995) A non-selective cation current activated via the multifunctional Ca^{2+}-calmodulin-dependent protein kinase in human epithelial cells. *J Physiol* **488:**37–55.

Chan HC, Kaetzel MA, Gotter AL, Dedman JR, and Nelson DJ (1994) Annexin IV inhibits calmodulin-dependent protein kinase II-activated chloride conductance A novel mechanism for ion channel regulation. *J Biol Chem* **269:**32464–32468.

Chao AC, de Sauvage FJ, Dong YJ, Wagner JA, Goeddel DV, and Gardner P (1994) Activation of intestinal CFTR Cl^- channel by heat-stable enterotoxin and guanylin via cAMP-dependent protein kinase. *EMBO J* **13:**1065–1072.

Cuthbert AW (2006) The prospects of pharmacotherapy for cystic fibrosis. *J R Soc Med* **99:**30–35.

Eggermont J (2004) Calcium-activated chloride channels: (un)known, (un)loved? *Proc Am Thorac Soc* **1:**22–27.

Farthing MJ (2006) Antisecretory drugs for diarrheal disease. *Dig Dis* **24:**47–58.

Galietta LJV, Haggie PM, and Verkman AS (2001) Green fluorescent protein-based halide indicators with improved chloride and iodide affinities. *FEBS Lett* **499:**220–224.

Gewald K and Hofmann I (1969) Heterocycles from CH-acid nitriles XV Reaction of ketones with cyanoacetic acid hydrazide and sulfur. *J Prakt Chem* **311:**402–407.

Gyömörey K, Garami E, Galley K, Rommens JM, and Bear CE (2001) Non-CFTR chloride channels likely contribute to secretion in the murine small intestine. *Pflugers Arch* **443 (Suppl 1):**S103–S106.

Hartzell C, Putzier I, and Arreola J (2005a) Calcium-activated chloride channels. *Annu Rev Physiol* **67:**719–758.

Hartzell C, Qu Z, Putzier I, Artinian L, Chien LT, and Cui Y (2005b) Looking chloride channels straight in the eye: bestrophins, lipofuscinosis and retinal degeneration. *Physiol (Bethesda)* **20:**292–302.

Hegab AE, Sakamoto T, Nomura A, Ishii Y, Morishima Y, Iizuka T, Kiwamoto T, Matsuno Y, Homma S, and Sekizawa K (2007) Niflumic acid and AG-1478 reduce cigarette smoke-induced mucin synthesis: the role of hCLCA1. *Chest* **131:**1149–5116.

Jayaraman S, Haggie P, Wachter R, Remington SJ, and Verkman AS (2000) Mechanism and cellular applications of a green fluorescent protein-based halide sensor. *J Biol Chem* **275:**6047–6050.

Kidd JF and Thorn P (2000) Intracellular Ca^{2+} and Cl^- channel activation in secretory cells. *Annu Rev Physiol* **62:**493–513.

Loewen ME and Forsyth GW (2005) Structure and function of CLCA proteins. *Physiol Rev* **85:**1061–1092.

Lorrot M and Vasseur M (2007) How do the rotavirus NSP4 and bacterial enterotoxins lead differently to diarrhea? *Virol J* **4:**31.

Ma T, Thiagarajah JR, Yang H, Sonawane ND, Folli C, Galietta LJ, and Verkman AS (2002a) Thiazolidinone CFTR inhibitor identified by high-throughput screening blocks cholera toxin-induced intestinal fluid secretion. *J Clin Invest* **110:**1651–1658.

Ma T, Vetrivel L, Yang H, Pedemonte N, Zegarra-Moran N, Galietta LJ, and Verkman AS (2002b) High-affinity activators of CFTR chloride conductance identified by high-throughput screening. *J Biol Chem* **277:**37235–37241.

Morris AP and Frizzell RA (1993) Ca^{2+}-dependent Cl^- channels in undifferentiated human colonic cells (HT-29) II Regulation and rundown. *Am J Physiol* **264:**C977–C985.

Morris AP, Scott JK, Ball JM, Zeng CQ, O'Neal WK, and Estes MK (1999) NSP4 elicits age-dependent diarrhea and Ca^{2+} mediated I^- influx into intestinal crypts of CF mice. *Am J Physiol* **277:**G431–G544.

Muanprasat C, Sonawane ND, Salinas D, Taddei A, Galietta LJ, and Verkman AS

(2004) Discovery of glycine hydrazide pore-occluding CFTR inhibitors: mechanism, structure-activity analysis, and in vivo efficacy. *J Gen Physiol* **124:**125–137.
Nilius B, Prenen J, Szucs G, Wei L, Tanzi F, Voets T, and Droogmans G (1997) Calcium-activated chloride channels in bovine pulmonary artery endothelial cells. *J Physiol* **498:**381–386.
Pedemonte N, Lukacs GL, Du K, Zegarra-Moran O, Galietta LJ, and Verkman AS (2005) Small molecule correctors of defective ΔF508-CFTR cellular processing identified by high-throughput screening. *J Clin Invest* **115:**2564–2571.
Rufo PA, Lin PW, Andrade A, Jiang L, Rameh L, Flexner C, Alper SL, and Lencer WI (2004) Diarrhea-associated HIV-1 APIs potentiate muscarinic activation of Cl^- secretion by T84 cells via prolongation of cytosolic Ca^{2+} signaling. *Am J Physiol Cell Physiol* **264:**C998–C1008.
Schultheiss G, Hennig B, Schunack W, Prinz G, and Diener M (2006) Histamine-induced ion secretion across rat distal colon: involvement of histamine H1 and H2 receptors. *Eur J Pharmacol* **546:**161–170.
Schultheiss G, Siefjediers A, and Diener M (2005) Muscarinic receptor stimulation activates a Ca^{2+}-dependent Cl^- conductance in rat distal colon. *J Membr Biol* **204:**117–127.
Seligman RB, Bost RW, and McKee RL (1953) Derivatives of p-aminosalicylic acid. *J Am Chem Soc* **75:**6334–6335.
Sridhar M, Raoa RM, Babaa NH, Kumbharea RM (2007) Microwave-accelerated Gewald reaction Synthesis of 2-aminothiophenes. *Tetrahedron Lett* **48:**3171–3172.
Suzuki M (2006) The *Drosophila* tweety family: molecular candidates for large-conductance Ca^{2+}-activated Cl^- channels. *Exp Physiol* **91:**141–147.
Takahashi A, Sato Y, Shiomi Y, Cantarelli VV, Iida T, Lee M, and Honda T (2000) Mechanisms of chloride secretion induced by thermostable direct haemolysin of Vibrio parahaemolyticus in human colonic tissue and a human intestinal epithelial cell line. *J Med Microbiol* **49:**801–810.
Tarran R, Loewen ME, Paradiso AM, Olsen JC, Gray MA, Argent BE, Boucher RC, and Gabriel SE (2002) Regulation of murine airway surface liquid volume by CFTR and Ca^{2+}-activated Cl^- conductances. *J Gen Physiol* **120:**407–418.
Thiagarajah JR, Verkman AS (2005) New drug targets for cholera therapy. *Trends Pharmacol Sci* **26:**172–175.
Verkman AS (2004) Drug discovery in academia. *Am J Physiol Cell Physiol* **286:** C465–C374.
Verkman AS and Jayaraman S (2002) Fluorescent indicator methods to assay functional CFTR expression in cells. *Methods Mol Med* **70:**187–196.
Worrell RT and Frizzell RA (1991) CaMKII mediates stimulation of chloride conductance by calcium in T84 cells. *Am J Physiol* **260:**C877–C882.
Yang H, Shelat AA, Guy RK, Gopinath VS, Ma T, Du K, Lukacs GL, Taddei A, Folli C, Pedemonte N, et al. (2003) Nanomolar affinity small-molecule correctors of defective ΔF508-CFTR chloride channel gating. *J Biol Chem* **278:**35079–35085.
Yangthara B, Mills A, Chatsudthiapong V, Tradtrantip L, and Verkman AS (2007) Small-molecule vasopressin-2 receptor antagonist identified by a G-protein coupled receptor 'pathway' screen. *Mol Pharmacol* **72:**86–94.

Address correspondence to: Dr. Alan S. Verkman, 1246 Health Sciences East Tower, Box 0521, University of California, San Francisco CA 94143-0521. E-mail: alan.verkman@ucsf.edu